

---

# Adversarial Robustness through Regularization: A Second-Order Approach

---

Avery Ma<sup>1</sup> Fartash Faghri<sup>1</sup> Amir-massoud Farahmand<sup>1</sup>

## Abstract

Adversarial training is a common approach to improving the robustness of deep neural networks against adversarial examples. In this work, we propose a novel regularization approach as an alternative. To derive the regularizer, we formulate the adversarial robustness problem under the robust optimization framework and approximate the loss function using a second-order Taylor series expansion. Our proposed second-order adversarial regularizer (SOAR) is an upper bound based on the Taylor approximation of the inner-max in the robust optimization objective. We empirically show that the proposed method improves the robustness of networks on the CIFAR-10 dataset.

## 1. Introduction

Adversarial training (Madry et al., 2017) is the standard approach for improving the robustness of deep neural networks (DNN), or any other estimator, against adversarial attacks. It is a data augmentation method that adds adversarial examples to the training set and updates the network with newly added data points. Intuitively, this procedure encourages the DNN not to make the same mistakes against an adversary. By adding sufficiently enough adversarial examples, the network gradually becomes robust to adversarial attacks. Note that Schmidt et al. (2018) show that under a Gaussian data model, the sample complexity of robust generalization is  $\sqrt{d}$  times larger than that of standard generalization. They further suggest that current datasets (e.g., CIFAR-10) may not be large enough to attain higher adversarial accuracy. Being a data augmentation procedure, however, is an indirect way to improve the robustness of a DNN. An alternative, which we pursue here, is to define a regularizer that penalizes DNN parameters that are prone to adversarial attacks. Minimizing the regularized loss function leads to estimators that are robust to adversarial attacks.

<sup>1</sup>University of Toronto & Vector Institute, Toronto, Canada. Correspondence to: Avery Ma <ama@cs.toronto.edu>.

Adversarial training and the proposed method can both be understood in terms of robust optimization formulation for adversarial robustness (Ben-Tal et al., 2009; Madry et al., 2017; Wong & Kolter, 2018; Shaham et al., 2018; Sinha et al., 2017). In this formulation, one is seeking to find a parameter  $w$  that minimizes

$$\min_w \mathbb{E} \left[ \max_{\delta \in \Delta} \ell(X + \delta, Y; w) \right], \quad (1)$$

where  $\ell$  is the loss function and  $\Delta$  is the set from which an adversary can choose its attack (we formally define all relevant quantities in Section 3). Adversarial training can be understood as approximating the solution of the inner maximization by finding perturbations with some specific attack technique, e.g., 7-step PGD (Madry et al., 2017). This is then followed by gradient descent on the loss computed at the perturbed input  $x + \delta$ . Note that as the value of  $\max_{\delta \in \Delta} \ell(x + \delta, x; w)$  depends on  $w$ , the perturbation found for an older  $w$  may not be a good attack for a newer  $w$ .

Our proposed method is more direct. It is based on approximating the loss  $\ell(x + \delta, x; w)$  using its Taylor series expansion (i.e.,  $\ell(x + \delta) \approx \ell(x) + \nabla \ell(x)^\top \delta + \frac{1}{2} \delta^\top \nabla^2 \ell(x) \delta$ , for a second order expansion), and then upper bounding the inner maximization problem of (1) using the Taylor series approximation. That is, we approximately solve  $\max_{\delta \in \Delta} [\ell(x) + \nabla \ell(x)^\top \delta + \frac{1}{2} \delta^\top \nabla^2 \ell(x) \delta]$ . In our derivations, we use the second-order expansion of the loss function, which leads to an expansion that includes both gradient and Hessian of the loss function with respect to (w.r.t.) the input. We call the method *Second-Order Adversarial Regularizer (SOAR)* (not to be confused with the Soar cognitive architecture Laird 2012). There are several steps that should be taken before this idea becomes practical. We describe them in details in Section 4. Our contribution are

- We show that an over-parameterized linear regression model can be severely affected by an adversary, even though its loss function is zero. A regularization-based approach can robustify such a model, suggesting that one can in general use a regularization-based approach instead of adversarial training (Section 2).
- We derive a regularizer that approximates the inner maximization of the robust optimization formulation, hence help improving the robustness of learned model

against adversarial attacks (Section 4).

- We empirically study the proposed regularizer and show that training with such a regularizer can significantly improve the adversarial robustness of the network (Section 5). The suggested regularizer has smaller negative effect on the standard accuracy (clean data), compared to adversarial training based on PGD.

## 2. Linear Regression with Over-parametrized Model: A Motivating Example

We consider a linear regression problem with over-parameterized model in order to show the possibility of using explicit regularization, instead of adversarial training.

Consider a linear model  $f_w(x) = \langle w, x \rangle$  with  $x, w \in \mathbb{R}^d$ . Suppose that  $w^* = (1, 0, 0, \dots, 0)^\top$  and the distribution of  $x \sim p$  is such that it is confined on a 1-dimensional subspace  $\{(x_1, 0, 0, \dots, 0) : x_1 \in \mathbb{R}\}$ . So the density of  $x$  is  $p((x_1, \dots, x_d)) = p_1(x_1)\delta(x_2)\delta(x_3)\dots\delta(x_d)$ , where  $\delta(\cdot)$  is Dirac's delta function. This setup can be thought of as using an over-parameterized model that has many irrelevant dimensions with data that is only covering the relevant dimension of the input space.

Let us consider the standard squared error pointwise loss  $l(x; w) = \frac{1}{2} |\langle x, w \rangle - \langle x, w^* \rangle|^2$ . Denote the residual by  $r(x; w) = \langle x, w - w^* \rangle$ . The population loss is  $L(w) = \mathbb{E}[l(X; w)] = \frac{1}{2} \mathbb{E}[|\langle X, w \rangle - \langle X, w^* \rangle|^2]$ .

Suppose that we use gradient descent (GD) to find the minimizer of this loss function. Furthermore, let us assume that we compute the gradient based on the population loss, instead of the empirical loss, in order to avoid any finite sample concern. We initialize the weights at the first time step as  $w(0) \sim N(0, \sigma^2 \mathbf{I}_{d \times d})$ , though the conclusions would not change much with other distributions. The GD procedure updates the weights according to  $w(t+1) \leftarrow w(t) - \beta \nabla_w L(w)$

The partial derivatives are

$$\frac{\partial L(w)}{\partial w_j} = \begin{cases} \int (w_1 - w_1^*) p_1(x_1) x dx = (w_1 - w_1^*) \mu_1, \\ \int (w_j - w_j^*) \delta(x_j) x dx = (w_j - w_j^*) 0 = 0, j \neq 1. \end{cases}$$

where  $\mu_1 = \mathbb{E}[X_1]$ . Notice that the gradient in dimension  $j = 1$  is non-zero, unless  $(w_1 - w_1^*) \mu_1 = 0$ . Assuming that  $\mu_1 \neq 0$ , this implies that the gradient won't be zero unless  $w_1 = w_1^*$ . On the other hand, the gradients in dimensions  $j = 2, \dots, d$  are all zero, so the GD procedure does not change the value of  $w_j(t)$  for  $j = 2, \dots, d$ . Therefore, under the proper choice of learning rate  $\beta$ , we get that the asymptotic solution of GD solution is  $\bar{w} \triangleq \lim_{t \rightarrow \infty} w(t) = (w_1^*, w_2(0), w_3(0), \dots, w_d(0))^\top$ .

We make two observations. The first is that  $L(\bar{w}) = 0$ , i.e.,

the population loss is zero. So from the perspective of training under the original loss, we are finding the right solution, even though the weights in dimensions 2 to  $d$  are the same as the randomly selected initial weights. The second observation is that we can easily attack this model by perturbing  $x$  by  $\Delta x = (0, \Delta x_2, \Delta x_3, \dots, \Delta x_d)^\top$ . The pointwise loss at  $x + \Delta x$  is

$$\begin{aligned} l(x + \Delta x; w) &= \frac{1}{2} |(w_1 - w_1^*) x_1 + \langle w, \Delta x \rangle|^2 \\ &= \frac{1}{2} |r(x; w) + \langle w, \Delta x \rangle|^2. \end{aligned}$$

With the choice of  $\Delta x_i = \varepsilon \text{sign}(w_i(0))$  (for  $i = 2, \dots, d$ ) and  $\Delta x_1 = 0$ , an FGSM-like attack (Goodfellow et al., 2014) at the learned weight  $\bar{w}$  leads to the pointwise loss of

$$l(x + \Delta x; \bar{w}) = \frac{1}{2} \varepsilon^2 \left[ \sum_{j=2}^d |w_j(0)| \right]^2 \approx \frac{1}{2} \varepsilon^2 \|w(0)\|_1^2.$$

In order to get a better sense of this loss, we compute its expected value w.r.t. the randomness of weight initialization. We have that (including the extra  $|w_1(0)|$  term too)

$$\begin{aligned} \mathbb{E}_{W \sim N(0, \sigma^2 \mathbf{I}_{d \times d})} [\|W\|_1^2] &= \mathbb{E} \left[ \sum_{i,j=1}^d |W_i| |W_j| \right] = \\ &= \sum_{i=1}^d \mathbb{E} [|W_i|^2] + \sum_{i,j=1, i \neq j}^d \mathbb{E} [|W_i|] \mathbb{E} [|W_j|], \end{aligned}$$

where we used the independence of the r.v.  $W_i$  and  $W_j$  when  $i \neq j$ . The expectation  $\mathbb{E} [|W_i|^2]$  is the variance  $\sigma^2$  of  $W_i$ . The r.v.  $|W_j|$  has a folded normal distribution, and its expectation  $\mathbb{E} [|W_j|]$  is  $\sqrt{\frac{2}{\pi}} \sigma$ . Thus, we get that

$$\mathbb{E}_{W \sim N(0, \sigma^2 \mathbf{I}_{d \times d})} [\|W\|_1^2] = d\sigma^2 + d(d-1) \frac{2}{\pi} \sigma^2 \approx \frac{2}{\pi} d^2 \sigma^2,$$

for  $d \gg 1$ . The expected population loss of the specified adversarial attack  $\Delta x$  at the asymptotic solution  $\bar{w}$  is

$$\mathbb{E}_{X, W} [l(X + \Delta x; \bar{w})] \approx O(\varepsilon^2 d^2 \sigma^2).$$

We see that when the dimension is large, this loss can be quite significant. The culprit here is that the GD procedure does not force the initial weights of this over-parameterized model to go to zero when there is no data from irrelevant to the task (or unused) dimensions.

The conventional strategy to increase the robustness of an estimator against adversarial attacks is through adversarial training, which is to add the adversarial examples to the training data and retraining the estimator. In this example, the adversarial training recipe suggests adding data points in the form of  $x + \Delta x =$

$(x_1, \varepsilon \text{sign}(w_2(0)), \dots, \varepsilon \text{sign}(w_d(0)))^\top$  to the training set (assuming we are using a finite training set as opposed to the population gradient). Even though this is feasible, and is in fact the standard approach, it may not be considered an elegant approach for this particular problem.

A more elegant approach, one may argue, is to notice that the reason an adversary can attack the learned model is that GD did not make the weights of irrelevant dimensions go to zero. This suggests that one might use some form of regularization in order to encourage the weights of irrelevant dimensions going to zero. A generic regularizer is to use the  $\ell_2$ -norm of the weights, i.e., formulate the problem as a ridge regression. In that case, the regularized population loss is

$$L_{\text{ridge}}(w) = \frac{1}{2} \mathbb{E} \left[ |\langle X, w \rangle - \langle X, w^* \rangle|^2 \right] + \frac{\lambda}{2} \|w\|_2^2.$$

One can see that the solution of  $\nabla_w L_{\text{ridge}}(w) = 0$  is  $\bar{w}_1(\lambda) = \frac{\mu_1}{\mu_1 + \lambda} w_1^*$  and  $\bar{w}_j(\lambda) = 0$  for  $j \neq 1$ . The use of this generic regularizer seems reasonable in this example, but we may wonder if it is possible to define a regularizer that is specially-designed for improving the adversarial robustness. This is what we do here in order to motivate the general development in Section 4.

Let us assume that a particular adversary attacks the model by adding  $\Delta x = (0, \varepsilon \text{sign}(w_2(0)), \dots, \varepsilon \text{sign}(w_d(0)))^\top$ . The expected loss is then

$$\begin{aligned} L_{\text{robustified}}(w) &\triangleq \mathbb{E} [l(X + \Delta x; w)] = \\ &\frac{1}{2} \mathbb{E} \left[ \left| r(x; w) + \varepsilon \sum_{j=2}^d |w_j| \right|^2 \right] = \\ L(w) + \varepsilon^2 \|w_{2:d}\|_1^2 + \varepsilon \mathbb{E} [r(X; w)] \|w_{2:d}\|_1, \end{aligned} \quad (2)$$

where  $\|w_{2:d}\|_1 = \sum_{j=2}^d |w_j|$ .<sup>1</sup> Minimizing  $L_{\text{robustified}}(w)$  is the same as minimizing the model at the point  $x' = x + \Delta x$  of the adversarial perturbation. The new regularizer  $\varepsilon^2 \|w_{2:d}\|_1^2 + \varepsilon \mathbb{E} [r(X; w)] \|w_{2:d}\|_1$  already incorporates the effect of adversary in exact form.

Nonetheless, there are two limitations of this approach. The first one is that it is designed for a particular choice of adversarial attack, an FGSM-like one. We would like a regularizer that is robust to a larger class of attacks. The second is that this regularizer is designed for a linear model and squared loss. How can we design a regularizer that can be used for more complicated models, such as DNNs? We address these questions by formulating the problem of adversarial robustness within the robust optimization framework (Section 3), and propose an approach to approximately solve it (Section 4).

<sup>1</sup>A similar, but more complicated result, would hold if the adversary could also attack the first dimension.

### 3. Robust Optimization Formulation for Adversarial Robustness

Designing an adversarial robust estimator can be formulated as a robust optimization problem, as shown by (Madry et al., 2017; Wong & Kolter, 2018). To describe it, let us introduce our notations first. Consider an input space  $\mathcal{X} \subset \mathbb{R}^d$ , an output space  $\mathcal{Y}$ , and a parameter (or hypothesis) space  $\mathcal{W}$ , which parameterizes a model  $f: \mathcal{X} \times \mathcal{W} \rightarrow \mathcal{Y}$ . In the supervised learning scenario, we are given a dataset in the form of  $\mathcal{D}_n = \{(X_i, Y_i)\}_{i=1}^n$  with  $(X_i, Y_i) \sim \mu$ . Given the prediction of  $f(x; w)$  and a target value  $y$ , the pointwise loss function of the model is denoted by  $\ell(x, y; w) \triangleq \ell(f(x; w), y)$ . Examples of the loss functions are the squared error for the regression problem and the cross-entropy loss for classification problem. Given the distribution of data, one can define the population loss (or risk) as  $L(w) = \mathbb{E} [\ell(X, Y; w)]$ . The goal of the standard supervised learning problem is to use the dataset  $\mathcal{D}_n$  in order to find a  $w \in \mathcal{W}$  that minimizes the population loss. A generic approach to do this is through empirical risk minimization (ERM). In order to control the complexity of the hypothesis, thus avoiding over- or under-fitting, regularization, explicitly or implicitly, is often used (Györfi et al., 2002; Steinwart & Christmann, 2008).

As shown in the previous section, it is possible to find a parameter  $w$  that makes this loss function very small, but leads to a model that is quite vulnerable to adversarial attacks. In order to improve the robustness of an estimator to adversarial attacks, we should be looking for parameters that make the loss function small while being robust to adversarial perturbations. We would like to put some constraints on the power of adversary (e.g., making sure that the amount of perturbation is not too large); otherwise, we cannot hope to have any robustness towards attacks. This can be specified by limiting that the adversary can only modify any input  $x$  to  $x + \delta$  with  $\delta \in \Delta \subset \mathcal{X}$ . Commonly used constraints are  $\varepsilon$ -balls w.r.t.  $\ell_p$ -norms, though other constraint sets have been used too (Wong et al., 2019). This goal can be formulated as a robust optimization problem where the objective is to minimize the adversarial population loss given some perturbation constraint  $\Delta$ :

$$\min_w \mathbb{E}_{(X, Y) \sim \mu} \left[ \max_{\delta \in \Delta} \ell(X + \delta, Y; w) \right]. \quad (3)$$

We have an interplay between two goals: 1) the inner-max term looks for the worst-case loss around the input, while 2) the outer-min term optimizes the hypothesis by minimizing such a risk.

The adversarial training can be intuitively understood as an approximation of this min-max problem. Instead of solving the inner-max problem, which is often computationally difficult, one may approximate it with another loss

that is obtained from a particular attack, perhaps under some computational budget. If we denote the perturbation generated by a particular adversary at  $x$  by  $\hat{\delta}(x)$ , we are effectively approximating  $\max_{\delta \in \Delta} \ell(x + \delta, y; w)$  by  $\ell(x + \hat{\delta}(x), y; w)$ . It is clear that for any  $\hat{\delta} \in \Delta$ , we have  $\mathbb{E} \left[ \ell(X + \hat{\delta}(X), Y; w) \right] \leq \mathbb{E} \left[ \max_{\delta \in \Delta} \ell(X + \delta, Y; w) \right]$ .

A common class of adversarial attacks are gradient-based attacks, such as FGSM, BIM and PGD, that utilize gradient (first-order) information of the network to compute perturbations (Goodfellow et al., 2014; Kurakin et al., 2016; Madry et al., 2017). They are simple and very effective attack techniques, especially when the perturbation is  $\ell_p$ -bounded. In particular, it has been shown that local loss maxima found by PGD have similar loss values, even with a large number of random restarts (Madry et al., 2017). This observation motivates the use of such attack method to approximate the solution of the inner-max problem.

As shown in Section 2, one can design a regularizer that provides the value of the loss function at the adversarially-attacked point, cf. (2). In that section, we focused on a particular model, loss function, and adversary. Such a regularizer relieved us from using a separate inner optimization procedure, as is done in adversarial training. Motivated by that example and the robust optimization framework discussed in this section, we devise a regularizer that approximates the robust formulation without much computational overhead. This may also provide us with some insight on how the adversary can be avoided, which is somewhat opaque in the adversarial training procedure.

#### 4. Second-Order Adversarial Regularizer (SOAR)

The main idea of SOAR is to approximate the loss function using Taylor series expansion around an input  $x$  and then solve the inner maximization term of the robust optimization formulation (3) using the approximated form. Describing this idea in detail is the topic of this section.

Assuming that the loss is twice differentiable, we can approximate the loss function around input  $x$  by the second-order Taylor expansion

$$\ell(x + \delta) \approx \ell(x) + \nabla \ell(x)^\top \delta + \frac{1}{2} \delta^\top \nabla^2 \ell(x) \delta. \quad (4)$$

Here we drop  $w$  and  $y$  in the original loss formulation to simplify the notation. It is important to realize that the gradients are computed with respect to the input  $x$ , i.e.,  $\nabla_x \ell(x)$  and  $\nabla_x^2 \ell(x)$ .

Let us focus on the  $\ell_p$  attacks, where the constraint set in (3) is  $\Delta = \{\delta : \|\delta\|_p \leq \varepsilon\}$  for some  $\varepsilon > 0$  and  $p \geq 1$ . In particular, let us focus on the  $\ell_\infty$  attacks. Using the second-

order Taylor series expansion, the inner optimization is

$$\max_{\|\delta\|_\infty \leq \varepsilon} \ell(x) + \nabla \ell(x)^\top \delta + \frac{1}{2} \delta^\top \nabla^2 \ell(x) \delta.$$

This Boolean quadratic programming (BQP) problem, however, is NP-hard (Beasley, 1998; Lima & Grossmann, 2017). Even though there exist semi-definite programming (SDP) relaxations, such approaches require the exact input Hessian, which is computationally expensive to obtain for high-dimensional inputs. And even if we could compute the exact Hessian, SDP itself is a computationally expensive approach, and perhaps not suitable to be within the inner loop of a DNN training. As such, we relax the  $\ell_\infty$  constraint to an  $\ell_2$  constraint, which as we shall see, leads to a computationally efficient solution. Note that with  $\delta \in \mathbb{R}^d$ , an  $\ell_\infty$  ball of size  $\varepsilon$  is enclosed by an  $\ell_2$ -ball of size  $\sqrt{d}\varepsilon$  with the same centre. Therefore, we can upper bound the inner maximization by

$$\max_{\|\delta\|_\infty \leq \varepsilon} \ell(x + \delta) \leq \max_{\|\delta\|_2 \leq \sqrt{d}\varepsilon} \ell(x + \delta), \quad (5)$$

which after substituting the second-order Taylor series expansion leads to an  $\ell_2$ -constrained quadratic optimization problem

$$\ell(x) + \max_{\|\delta\|_2 \leq \sqrt{d}\varepsilon} \left[ \nabla \ell(x)^\top \delta + \frac{1}{2} \delta^\top \nabla^2 \ell(x) \delta \right].$$

We could maximize each term inside the max separately and upper bound the max by  $\max_{\|\delta\|_2 \leq \sqrt{d}\varepsilon} \nabla \ell(x)^\top \delta + \max_{\|\delta\|_2 \leq \sqrt{d}\varepsilon} \frac{1}{2} \delta^\top \nabla^2 \ell(x) \delta = \sqrt{d}\varepsilon \|\nabla \ell(x)\|_2 + \frac{1}{2} d \varepsilon^2 \sigma_{\max}(\nabla^2 \ell(x))$ , where  $\sigma_{\max}(\nabla^2 \ell(x))$  is the largest singular value of the Hessian matrix,  $\nabla^2 \ell(x)$ . Even though the norm of the gradient and the singular value of the Hessian have an intuitive appeal, separately optimizing these terms might lead to a looser upper bound than necessary. The reason is that the maximizer of the first two terms are  $\arg\max |\nabla \ell(x)^\top \delta| = \frac{\nabla \ell(x)}{\|\nabla \ell(x)\|_2}$  and the direction corresponding to the largest singular value of  $\nabla^2 \ell(x)$ . In general, these two directions are not aligned. Solving the original optimization is easy though, and can be achieved by combine the expansion terms into a unified quadratic objective

$$\begin{aligned} \ell(x + \delta) &\approx \ell(x) + \frac{1}{2} \begin{bmatrix} \delta \\ 1 \end{bmatrix}^\top \begin{bmatrix} \nabla^2 \ell(x) & \nabla \ell(x) \\ \nabla \ell(x)^\top & 1 \end{bmatrix} \begin{bmatrix} \delta \\ 1 \end{bmatrix} - \frac{1}{2} \\ &= \ell(x) + \frac{1}{2} \delta'^\top \mathbf{H} \delta' - \frac{1}{2}, \end{aligned}$$

where  $\delta' = \begin{bmatrix} \delta \\ 1 \end{bmatrix}$  and  $\mathbf{H} = \begin{bmatrix} \nabla^2 \ell(x) & \nabla \ell(x) \\ \nabla \ell(x)^\top & 1 \end{bmatrix}$ . Note that  $\delta'$  is a  $d+1$ -dimensional vector and  $\mathbf{H}$  is a  $(d+1) \times (d+1)$  matrix.

This allows us to conveniently derive an upper bound on the expansion terms using the characteristics of a single Hessian term, and we arrive at the final objective with the perturbation in terms of  $\|\delta'\|_2$ :

$$\max_{\|\delta'\|_2 \leq \varepsilon'} \delta'^{\top} \mathbf{H} \delta' \quad (6)$$

with  $\varepsilon' = \sqrt{d\varepsilon^2 + 1}$ . To derive the regularizer, we use Cauchy-Schwarz inequality to obtain

$$\begin{aligned} \max_{\|\delta'\|_2 \leq \varepsilon'} \delta'^{\top} \mathbf{H} \delta' &\leq \max_{\|\delta'\|_2 \leq \varepsilon'} |\delta'^{\top} \mathbf{H} \delta'| \leq \\ \max_{\|\delta'\|_2 \leq \varepsilon'} \|\delta'\|_2 \|\mathbf{H} \delta'\|_2 &= \varepsilon' \max_{\|\delta'\|_2 \leq \varepsilon'} \|\mathbf{H} \delta'\|_2 = \varepsilon'^2 \|\mathbf{H}\|_2, \end{aligned} \quad (7)$$

where the last equality is obtained using properties of the  $\ell_2$ -induced matrix norm (this is the spectral norm). Since computing  $\|\mathbf{H}\|_2$  would again require the exact input Hessian, and we would like to avoid it, we calculate its upper bound. The spectral norm can be upper bounded by the Frobenius norm as  $\|\mathbf{H}\|_2 = \sigma_{\max}(\mathbf{H}) \leq \|\mathbf{H}\|_{\text{F}}$ . The Frobenius norm itself satisfies

$$\|\mathbf{H}\|_{\text{F}} = \sqrt{\text{Tr}(\mathbf{H}^{\top} \mathbf{H})} = \mathbb{E} [\|\mathbf{H}z\|_2], \quad (8)$$

where  $z \sim \mathcal{N}(0, \mathbf{I}_{(d+1) \times (d+1)})$ . Therefore, we can estimate  $\|\mathbf{H}\|_{\text{F}}$  by sampling random vectors  $z$  and compute the sample average of  $\|\mathbf{H}z\|_2$ .

Let us take a closer look at  $\mathbf{H}z$ . By decomposing  $z = [z_d, z_1]^{\top}$ , we get that

$$\mathbf{H}z = \begin{bmatrix} \nabla^2 \ell(x) z_d + z_1 \nabla \ell(x) \\ \nabla \ell(x)^{\top} z_d + z_1 \end{bmatrix}.$$

The term  $\nabla^2 \ell(x) z_d$  in  $\mathbf{H}z$  is a matrix-vector product that can be computed using Finite Difference (FD) approximation

$$\nabla^2 \ell(x) z_d \approx \frac{\nabla \ell(x + h z_d) - \nabla \ell(x)}{h}.$$

Note that  $\mathbb{E} [\|z_d\|_2] = \sqrt{d}$  for our normally distributed  $z$ . This can be quite large for high dimensional data. To ensure that the approximation direction always has the same magnitude, we use the normalized  $\tilde{z}_d = \frac{z_d}{\|z_d\|_2}$  instead, and use the following FD approximation

$$\nabla^2 \ell(x) z_d \approx \|z_d\| \frac{\nabla \ell(x + h \tilde{z}_d) - \nabla \ell(x)}{h}. \quad (9)$$

There are a few remaining details related to the possibility of gradient masking, i.e., having a very close to zero gradient at  $x$  in the training data. This might cause a regularizer based on  $\|\mathbf{H}\|$  evaluated at  $x$  ineffective. We next study SOAR in the simple logistic regression setting, which reveals why we might observe gradient masking. Based on that insight, we provide the remaining details of the method afterwards in Section 4.2.

#### 4.1. SOAR for a Linear Classifier

Consider a linear classifier  $f : \mathbb{R}^d \times \mathbb{R}^d \rightarrow \mathbb{R}$  with  $f(x; w) = \phi(\langle w, x \rangle)$ , where  $x, w \in \mathbb{R}^d$  are the input and the weights, and  $\phi(\cdot)$  is the sigmoid function. Note that the output of  $f$  has the interpretation of being a probability. For the cross-entropy loss function  $\ell(x, y; w) = -[y \log f(x; w) + (1 - y) \log(1 - f(x; w))]$ , the gradient w.r.t. the input  $x$  is  $\nabla \ell(x) = (f(x; w) - y)w$  and the Hessian w.r.t. the input  $x$  is  $\nabla^2 \ell(x) = f(x; w)(1 - f(x; w))ww^{\top}$ .

The second-order Taylor series expansion (4) with the gradient and Hessian being evaluated at  $x$  is

$$\ell(x + \delta) \approx \ell(x) + r(x, y; w)w^{\top} \delta + \frac{1}{2}u(x; w)\delta^{\top} ww^{\top} \delta, \quad (10)$$

where  $r(x, y; w) = f(x; w) - y$  is the residual term describing the difference between the predicted probability and the correct label, and  $u(x; w) = f(x; w)(1 - f(x; w))$ . Note that  $u$  has a confidence interpretation, and is close to 0 whenever the classifier is predicting a value close to 0 or 1. The upper bound on the Taylor approximation to inner maximization (5) is

$$\begin{aligned} \ell(x) + \max_{\|\delta\|_2 \leq \sqrt{d}\varepsilon} \left[ r(x, y; w)w^{\top} \delta + \frac{1}{2}u(x; w)\delta^{\top} ww^{\top} \delta \right] = \\ \ell(x) + \varepsilon \sqrt{d} |r(x, y; w)| \|w\|_2 + \frac{d\varepsilon^2}{2} u(x; w) \|w\|_2^2. \end{aligned}$$

The regularization term is encouraging the norm of  $w$  to be small, weighted according to the residual  $r(x, y; w)$  and the uncertainty  $u(x; w)$ . Whenever the classifier is correct with a large confidence, both  $r$  and  $u$  would be close to zero. The result is that the effect of the regularizer would be diminished, i.e., the weights are no longer regularized. In such a case, the Taylor series expansion, computed using the gradient and Hessian evaluated at  $x$ , becomes an inaccurate approximation to the loss, and hence its maximizer is not a good solution to the inner maximization problem anymore.

Note that this does not mean that one cannot use Taylor series expansion to approximate the loss. In fact, by the mean value theorem, there exists an  $h^* \in (0, 1)$  such that the second-order Taylor expansion is exact:  $\ell(x + \delta) = \ell(x) + \nabla \ell(x)^{\top} \delta + \frac{1}{2} \delta^{\top} \nabla^2 \ell(x + h^* \delta) \delta$ . The issue is that if we compute the Hessian at  $x$  (instead of at  $x + h^* \delta$ ), our approximation might not be very good whenever the loss function is close to being flat at  $x$ . This suggests that we might consider computing the gradient not at  $x$ , but at another point.

#### 4.2. Avoiding Gradient Masking

The insight from the last section suggests a few heuristics in order to improve the quality of SOAR. The first is to

compute the gradient and Hessian information at a point slightly different from the data point  $x$ , to avoid the detrimental effect of gradient masking in the calculation of the regularization. The second is using a randomly selected  $h$  in the FD approximation of (9) that is not infinitesimally small. We explain these in the rest of this section.

The discussion in Section 4.1 shows that whenever the logistic regression classifier becomes very confident in its prediction (i.e.,  $f(x; w)$  becomes close to 0 or 1) and predicts the correct label too, the regularizer becomes close to zero, and hence ineffective. Note that having a close to zero gradient is not a good defence strategy because despite its apparent success against iterative optimization-based attacks, a method relying on the gradient masking can be easily circumvented (Athalye et al., 2018b). Our early experimental results with DNNs had also indicated that gradient masking occurred with SOAR when the gradient and Hessian were evaluated at  $x$ . To systematically study this, we measure the average value of the highest probability output over test set data, that is,  $\frac{1}{N} \sum_{n=1}^N \max_{i \in \{1, 2, \dots, c\}} P(x_n)_i$ , where  $P(x_n)_i$  represent the probability of class  $i$  given data  $x_n$ . The result is reported in Table 5 in the Appendix B.

To mitigate this issue, we evaluate the gradient and Hessian, through a FD approximation (9) at a point slightly different from the input data  $x$ . One approach is to randomly perturb  $x$  by a stochastic noise. That is, we evaluate the gradient and Hessian at  $x' = x + \eta$  with a randomly chosen  $\eta$  within the  $\ell_\infty$  ball of size  $\varepsilon$  (random initialization), where  $\eta = (\eta_1, \eta_2, \dots, \eta_d)^\top$  and  $\eta_i \sim \mathcal{U}(-\varepsilon, \varepsilon)$ . The other is to follow one step of PGD adversary and then evaluate the gradient and Hessian (through the FD approximation again). That is,  $x' = x + \eta + \varepsilon_{step} \nabla_x \ell(x + \eta)$  for (PGD1 initialization). We compare all variations in our experiments.

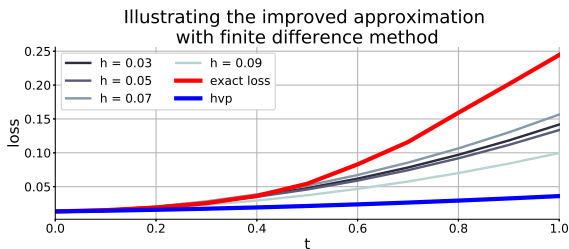


Figure 1. Consider a classifier trained via standard techniques (i.e. by minimizing the cross-entropy loss). We randomly select a point from the training set and apply random perturbation  $\eta$ . Suppose we have a linear interpolation between  $x$  and  $x + t\eta$  with  $t \in [0, 1.0]$ , we show (Red) the *exact* loss computed at the interpolated point:  $\ell(x + t\eta)$ , and the *approximated* loss through Taylor expansion. We consider two options for the second-order expansion term: (Blue) we use hessian vector product computed at the center of the expansion:  $\ell(x) + t\nabla\ell(x)^\top\eta + \frac{t^2}{2}\eta^\top\nabla^2\ell(x)\eta$ , and (Red) we use FD method  $\ell(x) + t\nabla\ell(x)^\top\eta + \frac{t^2\|\eta\|}{2}\eta^\top\frac{\nabla\ell(x+h\tilde{\eta})-\nabla\ell(x)}{h}$  with  $\tilde{\eta} = \frac{\eta}{\|\eta\|_2}$  and step size  $h$ .

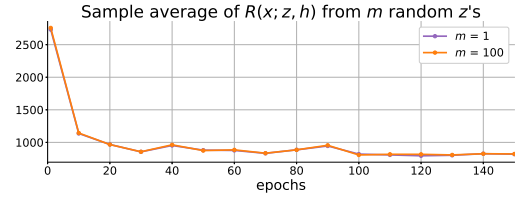


Figure 2. After each epoch, we compute the sample average of the regularizer in Equation 11 from 1 and 100 random directions  $z$ 's over the training set.

The second heuristic is related to the choice of step size  $h$  in the FD approximation (9). The conventional approach for FD method uses a very small  $h$  in computing the forward gradient. This leads to an accurate gradient computation. The analysis of Section 4.1, however, shows that whenever the classifier becomes very confident, the curvature profile obtained at the *exact* centre of the Taylor series may not lead to an accurate approximation of the loss under perturbation. By choosing a larger  $h$ , however, we compute the average slope or curvature over a larger domain, and can potentially avoid this issue. This is empirically shown in Figure 1, with more examples provided in the Appendix. We observe that the Taylor series approximation that uses the exact value of Hessian (i.e., no FD approximation) provides a poor approximation to the loss function of a DNN, while a FD approximation with a not very small  $h$  can in fact provide a better approximation. Based on these observations, we propose to randomly draw the step size  $h$  in our regularizer from a uniform distribution, i.e.,  $h \sim \mathcal{U}(0, \alpha)$  with an  $\alpha$  that is not too close to zero. Since sampling  $h$  from a uniform distribution can roughly be viewed as averaging the curvature from 0 to  $\alpha$ , this step might help in providing more meaningful second order information.

To summarize, the regularizer evaluated at  $x$ , with a direction  $z$ , and FD step size parameter  $h > 0$  is

$$R(x; z, h) = \frac{d\varepsilon^2 + 1}{2} \left\| \left[ \|z_d\|_2 \frac{\nabla\ell(x+h\tilde{z}_d) - \nabla\ell(x)}{h} + z_1 \nabla\ell(x) \right] \right\|_2, \quad (11)$$

with  $\tilde{z}_d = \frac{z_d}{\|z_d\|_2}$  being the normalized direction. The expectation in (8) can then be approximated by taking  $m$  samples of  $z_i$  drawn from  $z_i \sim \mathcal{N}(0, \mathbf{I}_{(d+1) \times (d+1)})$ . In practice, we observed that a single random direction provides a close approximation to the expectation. Figure 2 compares  $\frac{1}{n} \sum_{i=1}^n R(x_i, z_i)$  and  $\frac{1}{n} \sum_{i=1}^n \sum_{j=1}^m R(x_i, z_j)$  after each epoch, where the summation on  $i = 1, \dots, n$  is over the training data points  $X_i$ . Based on this observation, the regularized pointwise objective for a data point  $(x, y)$  is

$$\ell_{\text{SOAR}}(x, y) = \ell(x', y; w) + \lambda R(x'; z, h), \quad (12)$$

where  $z \sim \mathcal{N}(0, \mathbf{I}_{(d+1) \times (d+1)})$  and  $h \sim \mathcal{U}(0, \alpha)$  and the point  $x'$  is either equal to  $x$  (zero initialization), or  $x' =$

Table 1. Performance on CIFAR-10 against  $\ell_\infty$  bounded adversarial perturbations ( $\epsilon = 8/255$ ).

Method	Standard accuracy	FGSM	PGD7	PGD20
Standard	<b>86.33%</b> $\pm$ 0.42	22.09% $\pm$ 0.45	1.26% $\pm$ 0.16	0.39% $\pm$ 0.12
Adv7	70.71% $\pm$ 0.01	42.37% $\pm$ 0.27	38.52% $\pm$ 0.23	<b>36.03%</b> $\pm$ 0.16
Adv1-scratch	83.35% $\pm$ 0.19	27.84% $\pm$ 0.12	17.55% $\pm$ 0.35	13.14% $\pm$ 0.25
Adv1-pretrain	84.23% $\pm$ 0.17	23.13% $\pm$ 0.32	12.22% $\pm$ 0.16	8.11% $\pm$ 0.06
<b>SOAR</b>	<b>81.73%</b> $\pm$ 0.12	<b>47.77%</b> $\pm$ 0.29	<b>39.15%</b> $\pm$ 0.15	<b>32.83%</b> $\pm$ 0.15

$x + \eta$  (random initialization), or  $x' = x + \eta + \alpha \nabla_x \ell(x + \eta)$  (PGD1 initialization). We compare all variations in our experiments. The hyper-parameter  $\lambda$  should be equal to 1 based on the derivations, though we also observed that other values might lead to better performance.

## 5. Experiments

In this section, we verify the effectiveness of the proposed regularization method. Our experiments show that training with SOAR leads to a significant improvement in robustness under white-box and black-box  $\ell_\infty$  adversarial attacks as well as white-box  $\ell_2$  attacks. Unlike adversarial training, SOAR achieves robustness gain without a significantly sacrificing standard (average-case) accuracy. Our results against black-box attacks show no sign of gradient masking.

We evaluate SOAR on the CIFAR-10 dataset where the best defense against adversarial attacks is still adversarial training (Qin et al., 2019). We train a 4-layer CNN with ReLU non-linearities similar to a CNN used in Kingma & Ba (2014). Training data is augmented with random crops and horizontal flips. The Standard model is trained using only clean training data, for a total of 200 epochs with an initial learning rate of 0.01 and decay by an order of magnitude at epoch 100 and 150. SOAR refers to continuing the training of the Standard model with our regularizer in Equation 11. It is trained for a total of 150 epochs with an initial learning rate of 0.002 and decay at epoch 90 and 100. We set  $\lambda = 0.5$  and  $\alpha = 0.03$  for the regularizer. Adv7 is the adversarial training baseline trained only with 7-step PGD adversarial examples, it has an identical training schedule as the Standard model. All  $\ell_\infty$ -PGD adversarial examples used for training and evaluations are generated with  $\epsilon = 8/255$  and a step size of  $2/255$  (pixel values are normalized by 255 to the range  $[0, 1]$ ). Additional results against more attacks are discussed in Appendices D and E.

### 5.1. Robustness against White-Box Attacks

Table 1 compares the performance of SOAR to baselines against standard accuracy and white-box adversarial attacks. Training with SOAR significantly improves the adversarial robustness against FGSM and PGD7 while retain-

ing a higher standard accuracy compared to Adv7. Adv7 achieves only 3.2% higher accuracy against PGD20 than SOAR while we achieve 11% higher accuracy in standard accuracy and 5.4% higher accuracy against FGSM. Previous works have usually attributed the drop in standard accuracy to a trade-off between accuracy and robustness (Madry et al., 2017; Tsipras et al., 2018). However, even if such trade-off exists in real datasets, these results argue against a simply linear one.

To demonstrate that PGD1 initialization is not the primary drive for the improved robustness, we also perform adversarial training with 1-step PGD adversaries trained from random initialization (Adv1-scratch). Since the regularization is applied to pretrained models, we also include 1-step PGD adversarial training from pretrained models (Adv1-pretrain). Both methods perform poorly against PGD7 and PGD20 attacks that shows a failure in generalization to stronger attacks than ones used during training.

Table 2. Accuracy (%) against  $\ell_2$ -PGD attacks.

Method	$\epsilon = \frac{20}{255}$	$\epsilon = \frac{40}{255}$	$\epsilon = \frac{60}{255}$
Standard	60.2 $\pm$ 0.1	33.7 $\pm$ 0.1	18.1 $\pm$ 0.3
Adv7	68.3 $\pm$ 0.1	65.6 $\pm$ 0.2	62.9 $\pm$ 0.2
<b>SOAR</b>	<b>76.8</b> $\pm$ 0.1	<b>71.3</b> $\pm$ 0.1	<b>65.8</b> $\pm$ 0.0

We evaluate methods against  $\ell_2$  attacks in Table 2. We use 100 iterations and a step size of  $2.5\epsilon/100$  for  $\ell_2$ -PGD attacks. Interestingly, we find that training with SOAR leads to a significant robustness against  $\ell_2$  adversaries, exceeding Adv7 by 8.4% for  $\epsilon = \frac{20}{255}$ . This aligns with findings by Simon-Gabriel et al. (2019), that empirically showed adversarial robustness through regularization gains robustness against more than one norm-ball attack at the same time.

### 5.2. Robustness against Black-Box Attacks

As shown in Athalye et al. (2018a), many defenses only reach an illusion of robustness through methods collectively known as gradient masking or gradient obfuscation. These methods often fail against the attacks generated against an undefended independently trained model known as black-box attacks. Recent works (Tramèr et al., 2017; Ilyas et al., 2019) have developed hypotheses for the

success of black-box attacks. Table 3 shows our results against  $\ell_\infty$ -PGD attacks with 20 iterations. In addition to a CNN, we also test against attacks generated on ResNet18 (He et al., 2016). SOAR demonstrates significant robustness compared to Adv7. These results confirm that the robustness of SOAR is not due to gradient masking.

Table 3. Accuracy (%) against black-box  $\ell_\infty$ -PGD attacks ( $\epsilon = 8/255$ ).

Method\Source	CNN	ResNet18
Standard	$18.1 \pm 0.6$	$63.7 \pm 0.9$
Adv7	$68.3 \pm 0.1$	$69.9 \pm 0.1$
<b>SOAR</b>	<b><math>72.6 \pm 1.0</math></b>	<b><math>79.8 \pm 0.2</math></b>

## 6. Related Work

Adversarial training (Szegedy et al., 2013) was the first defense proposed against adversarial attacks along with their discovery. They used LBFGS to find adversarial examples for training. Goodfellow et al. (2014) proposed the Fast Gradient Sign Method (FGSM) to speed up the generation of adversarial examples during training where an epsilon times the sign of the gradient was used as an adversarial perturbation. The original experiments did not prove FGSM to be a complete solution to adversarial attacks. Madry et al. (2017) proposed adversarial training with iterative FGSM also known as PGD attacks. As Schott et al. (2018) noted, adversarial training has an important deficiency; it relies on a choice of norm-ball that fails to gain robustness against other norm-ball constraints. On MNIST, adversarial training with PGD does not do better than binarizing the image to black and white and on CIFAR10, there is still a significant gap between standard (average-case) accuracy and accuracy against adversarial attacks. Even worse, the robustness gained is at the cost of a big drop in standard accuracy. Recently, Wong et al. (2020) argued that training with FGSM attacks can be as strong as PGD if carefully done. Despite the shortcomings, adversarial training is still a competitive defense on MNIST and CIFAR-10 datasets (Hoffman et al., 2019). It is also one of the few methods that have survived tests against gradient masking (Athalye et al., 2018a).

Given the limitations of adversarial training, various alternatives have been studied. Adversarial regularization methods are the most related to our proposed method. We categorize these methods based on the order of Taylor approximation to the adversarial loss. TRADE (Zhang et al., 2019) regularizes only the output of the model and does not regularize gradients or the Hessian. It was designed to encourage smoothness of the loss function. They added a loss for the difference between the output of the model on a training data and its corresponding adversarial example. The subtle difference with adversarial training is to not use the

true target label in the regularization term.

Simon-Gabriel et al. (2019) studied the first order Taylor approximation to the adversarial loss. They proposed two future directions, direct regularization of the norm of the gradients as well as architectural modifications that result in smaller norm of gradients. However, simply reducing the norm of gradients can quickly lead to models with gradient masking. Hoffman et al. (2019) proposed Jacobian regularization by minimizing the Frobenius norm of the Jacobian. LLR (Qin et al., 2019) is another regularization based on the first order Taylor approximation of the adversarial loss. In contrast, they minimize the magnitude of the projection of gradient along a particular direction. The direction used is the one that maximizes the error of the first order Taylor approximation.

CURE (Moosavi-Dezfooli et al., 2019) is the closest to our method. They proposed directly minimizing the curvature of the loss function. They empirically observed that adversarial training leads to a reduction in the magnitude of eigenvalues of the Hessian with respect to the input. To reduce the computation time and numerical challenges, they regularized the model by the distance of gradients along the FGSM direction.

As experiments of Qin et al. (2019) show, none of these methods perform better than adversarial training on CIFAR-10 dataset. Our proposed method is the first regularization method that performs better than adversarial training on CIFAR-10 dataset.

## 7. Conclusion

This work proposed SOAR, a regularizer that improves the robustness of DNN to adversarial attacks. This is a more explicit alternative to adversarial training. SOAR was obtained using the second-order Taylor series approximation of the loss function w.r.t. the input, and approximately solving the inner maximization of the robust optimization formulation to the adversarial robustness. We showed that training with SOAR leads to adversarial robustness, with significant improvement in robustness under white-box and black-box  $\ell_\infty$  adversarial attacks as well as white-box  $\ell_2$  attacks. More importantly, SOAR achieves robustness gain without a significant trade-off with standard accuracy.

This is only a first step in designing better regularizers to improve the adversarial robustness. Several directions deserve further study. One direction is to understand the loss surface of DNN better in order to select a good point around which an accurate Taylor approximation can be made. This is important for designing regularizers that are not affected by gradient masking.



## References

- Athalye, A., Carlini, N., and Wagner, D. Obfuscated gradients give a false sense of security: Circumventing defenses to adversarial examples. *arXiv preprint arXiv:1802.00420*, 2018a. 7, 8
- Athalye, A., Carlini, N., and Wagner, D. Obfuscated gradients give a false sense of security: Circumventing defenses to adversarial examples. In *Proceedings of the 35th International Conference on Machine Learning*, pp. 274–283, 2018b. 6
- Beasley, J. E. Heuristic algorithms for the unconstrained binary quadratic programming problem. *London, England*, 1998. 4
- Ben-Tal, A., El Ghaoui, L., and Nemirovski, A. *Robust optimization*, volume 28. Princeton University Press, 2009. 1
- Engstrom, L., Tran, B., Tsipras, D., Schmidt, L., and Madry, A. Exploring the landscape of spatial robustness. In *Proceedings of the 36th International Conference on Machine Learning*, pp. 1802–1811, 2019. 12
- Ford, N., Gilmer, J., Carlini, N., and Cubuk, D. Adversarial examples are a natural consequence of test error in noise. *arXiv preprint arXiv:1901.10513*, 2019. 12
- Goodfellow, I. J., Shlens, J., and Szegedy, C. Explaining and harnessing adversarial examples. *arXiv preprint arXiv:1412.6572*, 2014. 2, 4, 8
- Györfi, L., Kohler, M., Krzyżak, A., and Walk, H. *A Distribution-Free Theory of Nonparametric Regression*. Springer Verlag, New York, 2002. 3
- He, K., Zhang, X., Ren, S., and Sun, J. Deep residual learning for image recognition. In *Proceedings of the IEEE conference on computer vision and pattern recognition*, pp. 770–778, 2016. 8
- Hoffman, J., Roberts, D. A., and Yaida, S. Robust learning with jacobian regularization. *arXiv preprint arXiv:1908.02729*, 2019. 8
- Ilyas, A., Santurkar, S., Tsipras, D., Engstrom, L., Tran, B., and Madry, A. Adversarial examples are not bugs, they are features. In *Advances in Neural Information Processing Systems*, pp. 125–136, 2019. 7
- Kingma, D. P. and Ba, J. Adam: A method for stochastic optimization. *arXiv preprint arXiv:1412.6980*, 2014. 7
- Kurakin, A., Goodfellow, I., and Bengio, S. Adversarial machine learning at scale. *arXiv preprint arXiv:1611.01236*, 2016. 4
- Laird, J. E. *The Soar cognitive architecture*. MIT press, 2012. 1
- Lima, R. M. and Grossmann, I. E. On the solution of non-convex cardinality boolean quadratic programming problems: a computational study. *Computational Optimization and Applications*, 66(1):1–37, 2017. 4
- Madry, A., Makelov, A., Schmidt, L., Tsipras, D., and Vladu, A. Towards deep learning models resistant to adversarial attacks. *arXiv preprint arXiv:1706.06083*, 2017. 1, 3, 4, 7, 8
- Moosavi-Dezfooli, S.-M., Fawzi, A., Uesato, J., and Frossard, P. Robustness via curvature regularization, and vice versa. In *Proceedings of the IEEE Conference on Computer Vision and Pattern Recognition*, pp. 9078–9086, 2019. 8
- Qin, C., Martens, J., Goyal, S., Krishnan, D., Dvijotham, K., Fawzi, A., De, S., Stanforth, R., and Kohli, P. Adversarial robustness through local linearization. In *Advances in Neural Information Processing Systems*, pp. 13824–13833, 2019. 7, 8
- Schmidt, L., Santurkar, S., Tsipras, D., Talwar, K., and Madry, A. Adversarially robust generalization requires more data. In *Advances in Neural Information Processing Systems*, pp. 5014–5026, 2018. 1
- Schott, L., Rauber, J., Bethge, M., and Brendel, W. Towards the first adversarially robust neural network model on mnist. *arXiv preprint arXiv:1805.09190*, 2018. 8
- Shaham, U., Yamada, Y., and Negahban, S. Understanding adversarial training: Increasing local stability of supervised models through robust optimization. *Neurocomputing*, 307:195–204, 2018. 1
- Simon-Gabriel, C.-J., Ollivier, Y., Bottou, L., Schölkopf, B., and Lopez-Paz, D. First-order adversarial vulnerability of neural networks and input dimension. In *International Conference on Machine Learning*, pp. 5809–5817, 2019. 7, 8
- Sinha, A., Namkoong, H., and Duchi, J. Certifying some distributional robustness with principled adversarial training. *arXiv preprint arXiv:1710.10571*, 2017. 1
- Steinwart, I. and Christmann, A. *Support Vector Machines*. Springer, 2008. 3
- Szegedy, C., Zaremba, W., Sutskever, I., Bruna, J., Erhan, D., Goodfellow, I., and Fergus, R. Intriguing properties of neural networks. *arXiv preprint arXiv:1312.6199*, 2013. 8

- Tramèr, F., Papernot, N., Goodfellow, I., Boneh, D., and McDaniel, P. The space of transferable adversarial examples. *arXiv preprint arXiv:1704.03453*, 2017. 7
- Tsipras, D., Santurkar, S., Engstrom, L., Turner, A., and Madry, A. Robustness may be at odds with accuracy. *arXiv preprint arXiv:1805.12152*, 2018. 7
- Wong, E. and Kolter, Z. Provable defenses against adversarial examples via the convex outer adversarial polytope. In *International Conference on Machine Learning*, pp. 5286–5295, 2018. 1, 3
- Wong, E., Schmidt, F. R., and Kolter, J. Z. Wasserstein adversarial examples via projected sinkhorn iterations. *arXiv preprint arXiv:1902.07906*, 2019. 3
- Wong, E., Rice, L., and Kolter, J. Z. Fast is better than free: Revisiting adversarial training. *arXiv preprint arXiv:2001.03994*, 2020. 8
- Zhang, H., Yu, Y., Jiao, J., Xing, E. P., Ghaoui, L. E., and Jordan, M. I. Theoretically principled trade-off between robustness and accuracy. *arXiv preprint arXiv:1901.08573*, 2019. 8

## A. Adversarial Robustness of the Model Trained using SOAR with Different Initializations

Table 4. Performance of SOAR on CIFAR-10 against  $\ell_\infty$  bounded adversarial perturbations ( $\varepsilon = 8/255$ ).

Method	Standard accuracy	PGD20	CNN	ResNet18
<b>SOAR</b>				
- zero init	84.28% $\pm$ 0.32	71.09% $\pm$ 0.93	15.10% $\pm$ 9.83	60.85% $\pm$ 1.16
- random init	83.85% $\pm$ 0.51	73.64% $\pm$ 0.24	20.97% $\pm$ 12.46	69.71% $\pm$ 0.60
- PGD1 init	81.73% $\pm$ 0.12	<b>32.83%</b> $\pm$ 0.15	<b>72.62%</b> $\pm$ 0.95	<b>79.79%</b> $\pm$ 0.16

We report the adversarial robustness of the model trained using SOAR with different initialization techniques in Table 4. The third column shows the accuracy against white-box PGD20 adversaries. The fourth and the fifth columns show the accuracy against black-box PGD20 adversaries transferred from models with different network designs. The source models are independently initialized and trained with clean data.

We notice that despite the high adversarial accuracy against white-box PGD attacks, models trained using SOAR with zero and random initialization perform poorly against transferred attacks. This suggests the presence of gradient masking when using SOAR with zero and random initializations. Evidently, SOAR with PGD1 initialization alleviates the gradient masking problem.

## B. Potential Causes of Gradient Masking

Table 5. Average value of the highest probability output for all test set data, that is,  $\frac{1}{N} \sum_{n=1}^N \max_{i \in \{1, 2, \dots, c\}} P(x_n)_i$ , where  $P(x_n)_i$  represent the probability of class  $i$  given data  $x_n$ .

Method	Standard	Random	PGD1
Standard	94.86% $\pm$ 0.16	94.18% $\pm$ 0.15	94.72% $\pm$ 0.28
Adv7	53.81% $\pm$ 0.13	53.63% $\pm$ 0.14	53.81% $\pm$ 0.12
Adv1-scratch	85.72% $\pm$ 0.19	85.61% $\pm$ 0.17	85.72% $\pm$ 0.14
Adv1-pretrain	87.46% $\pm$ 0.05	87.32% $\pm$ 0.04	87.46% $\pm$ 0.07
<b>SOAR</b>			
- zero init	99.63% $\pm$ 0.03	<b>99.61%</b> $\pm$ 0.03	99.82% $\pm$ 0.00
- random init	99.61% $\pm$ 0.02	<b>99.57%</b> $\pm$ 0.04	99.83% $\pm$ 0.01
- PGD1 init	93.85% $\pm$ 0.03	93.80% $\pm$ 0.02	93.31% $\pm$ 0.03

We summarize the average value of the highest probability output for test set data initialized with zero, random and PGD1 perturbations in Table 5. We notice that training with SOAR using zero or random initialization leads to models with nearly 100% confidence on their predictions. This is aligned with the analysis of SOAR for a linear classifier (Section 4.1), which shows that the regularizer becomes ineffective as the model outputs high confidence predictions. Indeed, results in Table 4 show that those models are vulnerable under black-box attacks.

Recall that PGD attacks involve initializing the clean data  $x_n$  with a randomly chosen  $\eta$  within the  $\ell_\infty$  ball of size  $\varepsilon$ , followed by gradient ascent at  $x_n + \eta$ . Results in Table 5 suggest that highly confident predictions could be an indication for gradient masking. Suppose that the model makes predictions with 100% confidence on any given input. This leads to a piece-wise loss surface that is either zero (correct predictions) or infinity (incorrect predictions). The gradient of this loss function is either zero or undefined making gradient ascent ineffective. Therefore, white-box gradient-based attacks are unable to find adversarial examples.

## C. Model & Training Details

**Hyperparameters for the CNN:** The four layer CNN model has kernel sizes = [3, 3, 3, 3], strides = [1, 1, 1, 1], and output channel size = [32, 32, 64, 64]. All layers use ReLU activation functions, and layer 2 and 4 are followed by max-pooling.

**Standard/Adversarial training:** We train the model for 200 epochs, with an initial learning rate of 0.01. We decay the

learning rate by an order of magnitude at epoch [100, 150]. We used a minibatch size of 128 for testing and training. We used SGD optimizer with momentum of 0.9 and a weight decay of  $2e-4$ .

**Regularization with SOAR:** We continue training from a pretrained the model for an additional 150 epochs, with an initial learning rate of 0.002, and an update schedule of [90, 100]. We used a minibatch size of 128 for testing and training. We used SGD optimizer with momentum of 0.9 and a weight decay of  $2e-4$ . The parameters for the regularizer are:  $\lambda = 0.5$  and  $\alpha = 8/255$ . We apply two types of clipping: a gradient clipping of 30 on the  $\ell_2$  norm of regularizer gradient, and a clipping of 10 on the value of the  $\ell_2$  norm part of the regularizer. The primary reason for the clipping operation is that at the beginning of the regularization, the loss gradient can be very small compared to the regularizer gradient.

**Reproducibility:** All necessary source code files and Jupyter notebooks are included to reproduce the results reported in this paper.

## D. Robustness under Image Transformation

Table 6. Robustness under different image transformations

Method	Weak	Medium	Strong
Standard	$83.07\% \pm 0.09$	$61.19\% \pm 1.04$	$35.89\% \pm 0.64$
Adv7	$69.87\% \pm 0.24$	$60.60\% \pm 0.13$	$32.51\% \pm 0.39$
SOAR	$80.51\% \pm 0.16$	$68.42\% \pm 0.47$	$38.04\% \pm 0.44$

To provide further evidence on the improved robustness with SOAR, we apply a more natural class of image perturbation such as translations and rotations. Compared to the previous evaluations, this type of image corruption is fundamentally different, because perturbations are not constrained by a specific norm metric. We consider a combination of random rotations and translations with three attack strengths: weak ( $\pm 10^\circ$ ,  $\pm 5\%$ px), medium: ( $\pm 30^\circ$ ,  $\pm 10\%$ px), and strong: ( $\pm 50^\circ$ ,  $\pm 30\%$ px). Engstrom et al. (2019) showed that the improved robustness through  $\ell_\infty$  Adv7 adversarial training is orthogonal to spatial robustness, which is aligned with our results shown in Table 6. They argue that it is possibly the result of overfitting to strong  $\ell_\infty$  adversarial examples through adversarial training. On the other hand, we notice that the improved adversarial robustness with SOAR translates to improved robustness against such non- $\ell_p$ -bounded perturbations.

## E. Robustness under Gaussian Noise

Table 7. Robustness of the model under additive Gaussian noise with different standard deviations

Method	$\sigma = 0.05$	$\sigma = 0.1$	$\sigma = 0.15$
Standard	$69.99\% \pm 1.06$	$36.42\% \pm 2.71$	$20.63\% \pm 1.76$
Adv7	$69.70\% \pm 0.25$	$65.52\% \pm 0.25$	$58.80\% \pm 0.36$
SOAR	$79.98\% \pm 0.26$	$71.34\% \pm 1.08$	$56.81\% \pm 2.61$

It is difficult to accurately measure model robustness with only a handful of adversarial attacks, because most attack methods rely on using model parameters to find perturbations, particularly in the case of white-box attacks. Ford et al. (2019) made the connection between adversarial robustness and robustness under Gaussian noise, and suggested evaluating robustness under a known distributional shift. Here, we verify the improved robustness of the proposed regularizer under additive  $d$ -dimensional spherical Gaussian noise with zero mean and unit variance. In a high dimensional space such as the one for CIFAR-10, perturbations sampled from  $\mathcal{N}(\mathbf{x}, \sigma^2 I)$  concentrate near the surface of the sphere with radius  $\sigma\sqrt{d}$ .

Robustness under additive Gaussian noise allows us to assess model robustness independent of the limiting factors of generating adversarial examples. We report the results in Table 7. We see improvements over all methods similar to improvements against the closely related  $\ell_2$  attacks in Table 2. While adversarial training using strong  $\ell_\infty$  adversaries overfits to the specific choice of the norm, regularization can improve robustness of the model in a more general sense.

## F. Additional Experiments

This appendix briefly reports the results of some additional experiments. Figure 3 shows the clean test data and PGD20 attack performance of the model under SOAR regularization during different stages of training. We report the result with various regularization coefficient  $\lambda$ , cf. (12).

Figure 4 provides additional examples generated similar to that in Figure 1. We observe that when there is no curvature at the *exact* centre of the Taylor series expansion, the approximation of the loss under perturbation is poor. With FD method with a larger  $h$ , we compute the average curvature over a larger domain, and thus avoid the issue.

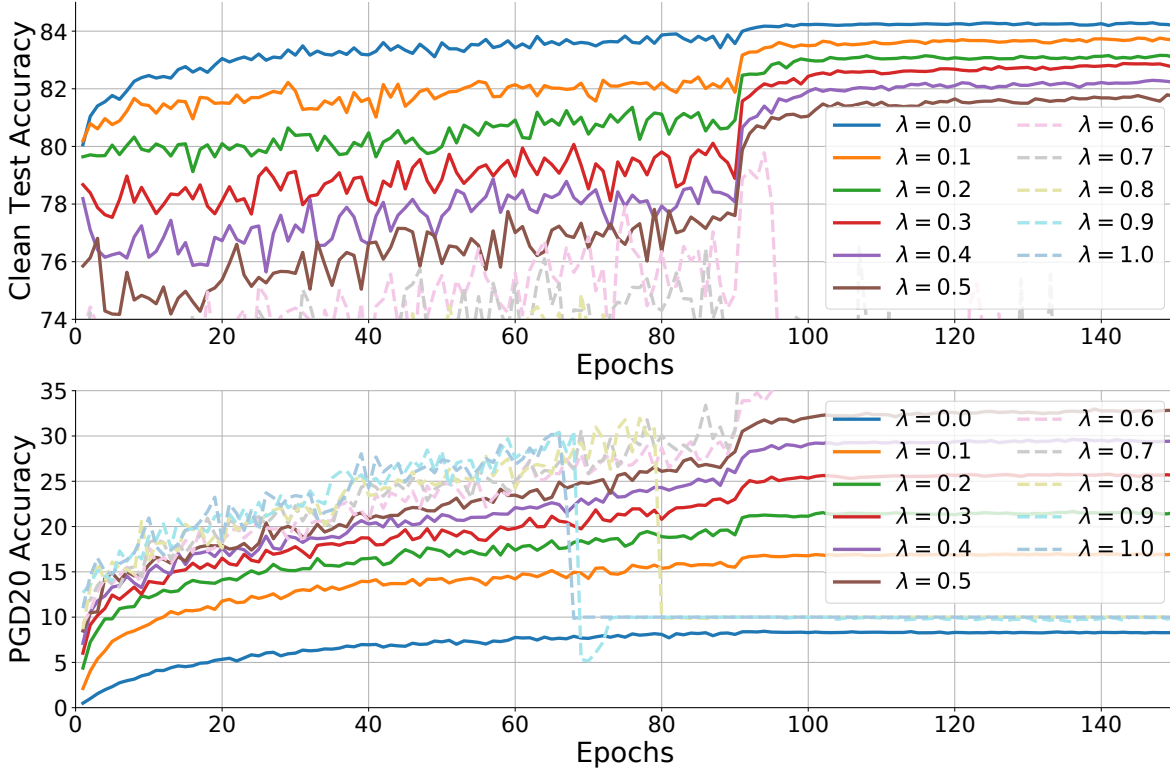


Figure 3. Improvement of adversarial robustness of the model under SOAR regularization. We illustrate the improved robustness under different  $\lambda$ . Top: Clean test accuracy. Bottom: Adversarial accuracy against white-box PGD20 adversaries. Recall the regularized pointwise objective for a data point  $(x, y)$  is  $\ell_{\text{SOAR}}(x, y) = \ell(x', y; w) + \lambda R(x'; z, h)$ . Note that with  $\lambda = 0$ , the training objective is equivalent to adversarial training with PGD1 adversaries.

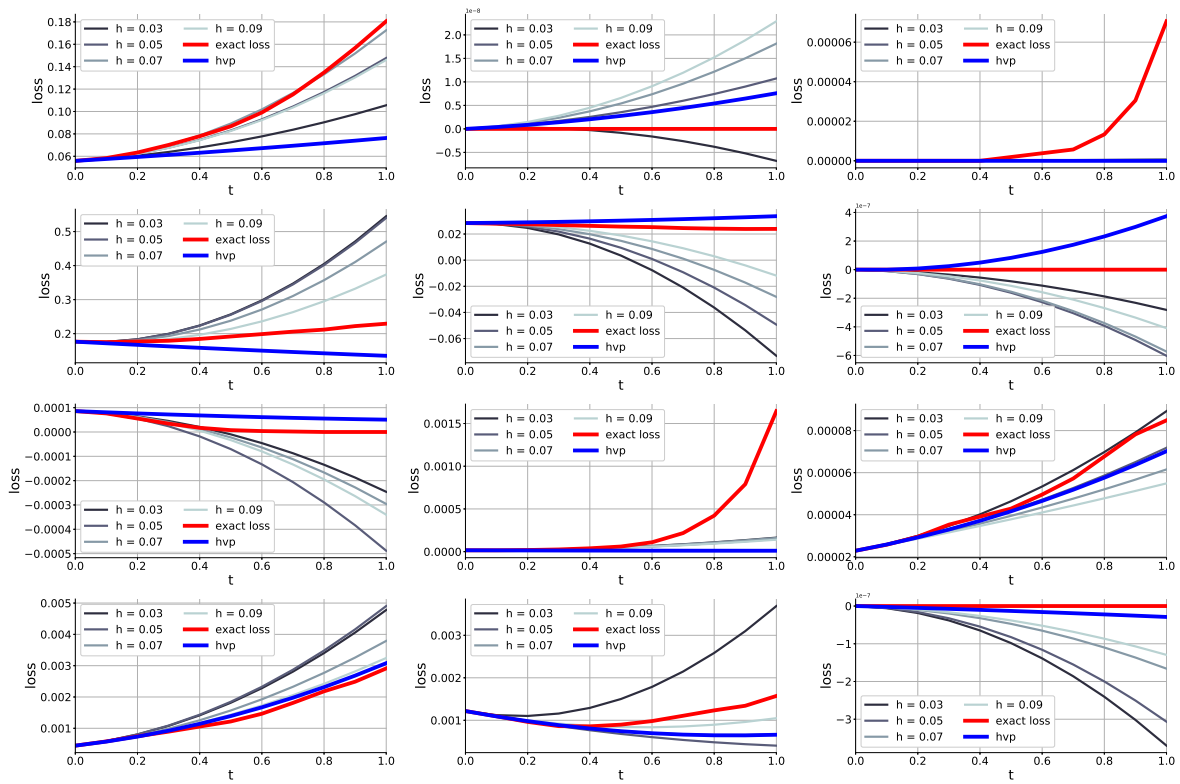


Figure 4. Additional examples similar to Figure 1 with different initial points.